



HAL
open science

Measurement of Electrolyte Resistance Fluctuations Generated by Oil-Brine Mixtures in a Flow-Loop Cell

Hanane Bouazaze, François Huet, Ricardo P. Nogueira

► **To cite this version:**

Hanane Bouazaze, François Huet, Ricardo P. Nogueira. Measurement of Electrolyte Resistance Fluctuations Generated by Oil-Brine Mixtures in a Flow-Loop Cell. *Corrosion*, 2007, 63, pp.307-317. hal-00139939

HAL Id: hal-00139939

<https://hal.science/hal-00139939>

Submitted on 6 May 2023

HAL is a multi-disciplinary open access archive for the deposit and dissemination of scientific research documents, whether they are published or not. The documents may come from teaching and research institutions in France or abroad, or from public or private research centers.

L'archive ouverte pluridisciplinaire **HAL**, est destinée au dépôt et à la diffusion de documents scientifiques de niveau recherche, publiés ou non, émanant des établissements d'enseignement et de recherche français ou étrangers, des laboratoires publics ou privés.



Distributed under a Creative Commons Attribution - NonCommercial 4.0 International License

Measurement of Electrolyte Resistance Fluctuations Generated by Oil-Brine Mixtures in a Flow-Loop Cell

H. Bouazaze*, F. Huet* and R.P. Nogueira**

ABSTRACT

Measurements of current and electrolyte-resistance fluctuations between two working electrodes in a flow-loop cell have been carried out with the objective to assess and/or monitor corrosion and characterize hydrodynamic flows in pipelines. Linear flow velocities of 1 m/s and 2 m/s were used to ensure different hydrodynamic conditions for oil-brine mixtures with a large range of volumetric oil content (VOC) from 0% to 80% (water-cut from 100% to 20%). Previous results obtained in conventional cylindrical cells, in which the oil-brine mixture was homogenized with a rotating magnet, have been confirmed. The current fluctuations present a very complex and nonmonotonic behavior with the VOC, which yields corrosion monitoring virtually impossible in these conditions. Conversely, the electrolyte-resistance fluctuations appeared to be a reliable and very sensitive tool for the real-time analysis of hydrodynamic conditions and flow composition that can be used for the indirect assessment of oil-brine corrosivity. The analysis of the mean electrolyte-resistance values has shown an excellent agreement with the theoretical predictions of Maxwell's model of the electrical conductivity in two-phase media over the whole VOC range investigated, provided that hydrodynamic conditions ensure the homogeneity of the mixture. Electrochemical measurements have been complemented with the analysis of video images that allowed identification of the oil/brine mixture structure close to the pipe wall and the

distribution function of the oil-droplet diameter, which were shown to be spherical for VOCs up to 60% (water-cut down to 40%).

KEY WORDS: conductivity, electrochemical noise, electrolyte resistance, image analysis, monitoring, oil/water, two-phase flow

INTRODUCTION

Measurements of electrochemical noise (EN)—current and potential fluctuations—in multiphase electrolytes have been carried out by several groups for monitoring corrosion processes.¹⁻⁷ Even if the EN depends on the composition and velocity of the multiphase flow, it is difficult to get relevant information on the corrosion processes because of the simultaneous contribution of the electrochemical and hydrodynamic effects in the measured current and potential signals.⁵ Moreover, in oil-brine mixtures of volume oil content (VOC), defined as the ratio $\phi = \text{oil volume}/\text{solution volume}$, ranging between 0% and 80%, which corresponds to a water-cut (WC) ranging between 100% and 20% ($\text{WC} = 1 - \text{VOC}$), the amplitude of the current and potential fluctuations were shown to vary non-monotonously within 1 or 2 decades, making difficult the interpretation of these variations with the VOC.^{5,7}

On the contrary, the electrolyte resistance (ER) fluctuations measured in the vicinity of a working electrode (WE) in oil-brine mixtures of various compositions stirred with a rotating magnet in a common cylindrical electrochemical cell have been shown to be much more sensitive to detect changes in the oil-brine composition close to the WE. Indeed, the amplitude of

* Corresponding author. E-mail: frh@ccr.jussieu.fr.

* UPR15 du CNRS, "Interfaces et Systèmes Electrochimiques," Université Pierre et Marie Curie, 4, place Jussieu, 75252 Paris Cedex 05, France.

** UMR5614 INPG-CNRS, "Thermodynamique et Physico-Chimie Métallurgiques," Institut National Polytechnique de Grenoble, BP 75, 38402 St. Martin d'Hères, France.

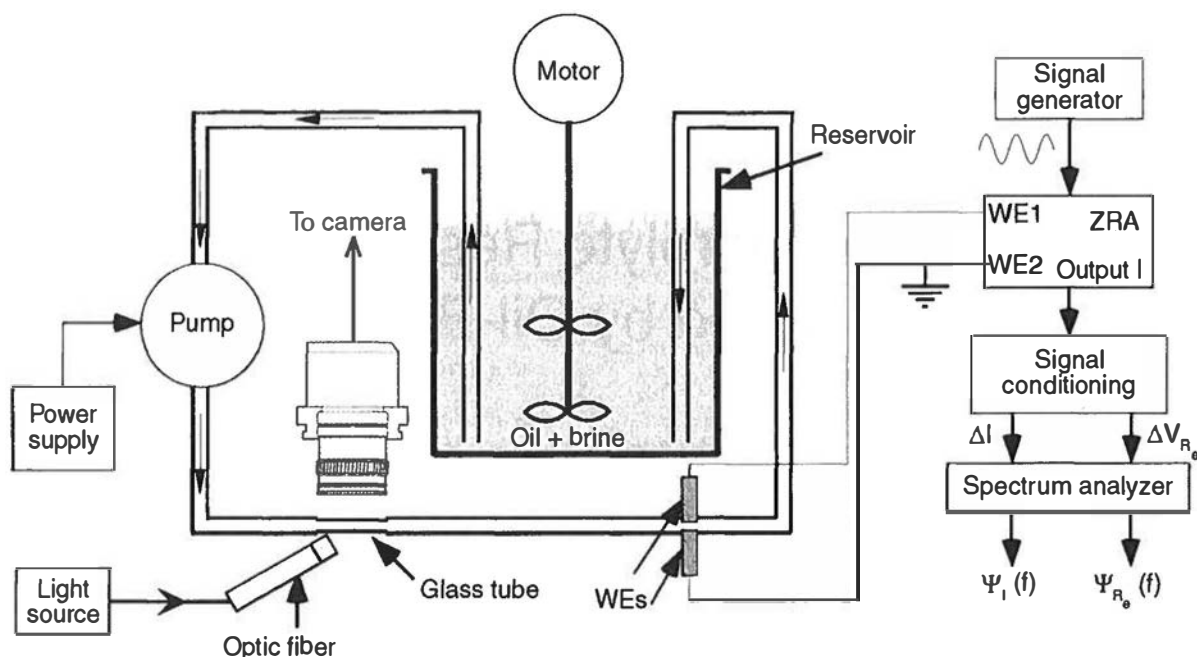


FIGURE 1. Experimental set-up used for measuring the current and ER fluctuations and filming the oil-brine mixture circulating in the flow-loop cell.

the ER fluctuations increased monotonously by a factor of 1,000 when the VOC increased from 0% to 80% (WC decreased from 100% to 20%).^{5,7}

This paper presents similar measurements of current and ER between two WEs in a flow-loop cell, first to approach conditions in pipelines with oil-brine solutions and second to compare the mean electrical conductivity of oil-brine mixtures to the theoretical values predicted by the Maxwell conduction model in heterogeneous systems.^{8,9} The theoretical and experimental values of the mean ER were not in good agreement for mixtures stirred in a cylindrical cell with a rotating magnet. This was attributed to a non-uniformity of the concentration of the oil droplets in the cell due to the formation of a vortex.⁷ Images of the mixtures have also been taken with a video camera at various VOC to investigate the influence of the electrolyte velocity on the size of the oil droplets and tentatively correlate the droplet size to the amplitude of the current and ER fluctuations.

EXPERIMENTAL PROCEDURES

Figure 1 presents the experimental set-up used for measuring the current and ER fluctuations between two WEs in a flow-loop cell and for imaging the oil-brine mixture. The electrolyte was a mixture of 3 wt% sodium chloride (NaCl) and paraffin oil (density: 0.87 g/cm^3 and kinematic viscosity: $\nu = 2.4 \text{ cm}^2/\text{s}$) prepared in the glass cylindrical reservoir (15 cm diameter and 20 cm height) used in the experiments. To obtain increasing values of VOC, the initial electrolyte

was a brine solution of 2 dm^3 , and different amounts of oil were successively added up to the total volume of the reservoir (3.5 dm^3). Then, the solution was replaced by a new solution of 2 dm^3 with the same VOC, and oil was progressively added. The procedure was repeated until a VOC of 80% was reached. At this high oil content, the mixture was likely a water-in-oil emulsion, but no attempt was made in this work to establish the VOC value beyond which the mixture flipped from oil-in-water to water-in-oil. This was the upper limit of the VOC used because local breakdowns of the electrical continuity of the mixture occurred above 80% and caused the interface control to temporarily switch off, as shown in a previous work.⁷ The solution was mixed in the reservoir with a double stirrer rotating at the maximum speed (450 rpm), avoiding electrolyte spilling outside the reservoir. No surfactant was used for stabilizing the mixture. Its circulation in the 4-m-long silicone pipe (inner diameter, $D = 1.5 \text{ cm}$) was ensured by a flexible-impeller pump (Bioblock C48144,[†] maximum flow rate: $46 \text{ dm}^3/\text{min}$, maximum direct current [DC] supply voltage: 24 V) without significant segregation of the oil and brine phases. Two different flow rates ($10.8 \text{ dm}^3/\text{min}$ and $20.4 \text{ dm}^3/\text{min}$ measured in the oil-free solution), corresponding to a DC supply voltage of 6 V and 14 V and to a flow velocity v of 1.0 m/s and 1.9 m/s, were investigated. For the lowest electrolyte velocity, the Reynolds number $Re = vD/\nu$ was about 15,000 in the oil-free solution ($\nu = 10^{-2} \text{ cm}^2/\text{s}$). Since the laminar-turbulent transition corresponds to a Re number between 2,000 and 4,000 for a single-phase solution, the flow was turbulent for the small VOC solutions. This might be different at high VOC

[†] Trade name.

values, since the viscosity of the solution, which was not measured in this work, increased with the VOC. The Reynolds number was about 60 for the brine-free solution, which means in the pure oily phase ($v = 1.0$ m/s). All experiments were performed at room temperature. Since the motor of the pump was slightly heating the circulating electrolyte, a rest period of 2 h was observed before the experiments to let the electrolyte temperature stabilize.

The WEs were the cross section of two identical, pure iron (99.99%) rods (0.5 cm in diameter) with their lateral surface isolated with a thin layer of a cathoporetic paint commonly used in the automotive industry for its anticorrosion properties. After polishing with emery paper up to 1,200 grit, the rods were inserted through the pipe. They protruded into the flow and faced each other at a distance of 0.8 cm or 1.0 cm, which could not be reproduced exactly for each experiment. A potentiostat used as a zero-resistance ammeter (ZRA) imposed a zero potential difference between the WEs so that their mean potential was the corrosion potential. Since this work was not aimed at measuring the noise resistance or the noise impedance of the electrodes, the fluctuations of the electrode potential were not measured so that no reference electrode was introduced in the channel. The ER between the WEs was measured with the help of a device especially conceived and developed for this task. This device, fully described elsewhere,^{7,10-11} is based on the following principle: a sinusoidal voltage signal, v_{hr} , with a frequency, $f_{hr} = 100$ kHz, at which the impedance of the WEs is reduced to the ER, R_c was superimposed to the zero potential difference imposed between the WEs. Its peak-to-peak amplitude was 140 mV when the VOC was between 0% and 70%, and 690 mV when the VOC was 80%. The current, I , flowing between the WEs had three components: the DC current (close to zero because the mean potential of the two WEs was the corrosion potential), the natural current fluctuations due to the corrosion processes, ΔI , and the sine wave current response, v_{hr}/R_c , at frequency f_{hr} . In the ER channel of the specific device, the first two components were eliminated with a high-pass filter while the third component, v_{hr}/R_c , was amplified, rectified with a diode, and low-pass-filtered to give a voltage signal, v_{R_c} , the amplitude of which was inversely proportional to the instantaneous value of the ER. The fluctuations of the ER induced voltage fluctuations, Δv_{R_c} , of v_{R_c} that could be easily obtained from the expression:

$$\Delta v_{R_c}(t) = b \Delta \left[\frac{1}{R_c(t)} \right] = -b \frac{\Delta R_c(t)}{\langle R_c \rangle^2} \quad (1)$$

where b is a proportionality factor (in $V \Omega$) obtained from a calibration procedure with a variable resistor in place of the electrochemical cell. The value of b was

18.801 $V \Omega$ for $0 \leq \phi \leq 70\%$ and 93.832 $V \Omega$ for $\phi = 80\%$. With the value of b and the mean value of v_{R_c} , the mean value $\langle R_c \rangle$ of the ER was also obtained. In the current channel of the specific device, the current response, v_{hr}/R_c , was eliminated with a low-pass filter and the current fluctuations, ΔI , were amplified, so that the specific device measured the ER and current fluctuations simultaneously.

The analog ER and current signals were digitized successively at different sampling frequencies (20 Hz, 200 Hz, and 2 kHz) with a real-time computer RTU 5450' with proper anti-aliasing low-pass filters after DC value elimination and amplification. The power spectral densities (PSDs) of the fluctuations of the signals were calculated between 10 mHz and 1 kHz with the help of the fast Fourier transform after Hann windowing.¹² To increase the accuracy of the PSDs, 10 time records were used for averaging 10 elementary PSDs at each sampling frequency. The measurement procedure was performed as follows:

- Two min after a new addition of oil in the reservoir, the mean value $\langle R_c \rangle$ of the ER was measured.
- The PSDs were then measured, which lasted about 20 min.
- The mean value $\langle R_c \rangle$ was measured again to evaluate its stationarity with time.

A charge-coupled device (CCD) video camera (Téli CS-3710/M,[†] resolution of 768 by 574 pixels) was used for imaging the oil-brine mixture through a glass pipe, replacing the silicone pipe at a distance of 16 cm above the WEs. The highest speed (1/10,000 s) of the electronic shutter of the camera was used to obtain sharp outlines of the oil droplets. The distribution function of the diameter of the droplets was estimated from a series of 60 images recorded every 40 ms for each VOC value. Each sharp droplet was analyzed individually; its diameter was determined by superposing a circle, the size of which was fixed manually, upon the droplet. Because of the opacity of the solution, which increased with the VOC, only the region close to the wall of the glass pipe could be imaged.

RESULTS AND DISCUSSION

Analysis of the Video Images of the Oil-Brine Mixture

Typical images of the mixture are given in Figure 2 for various VOCs at the electrolyte velocity of 1.0 m/s. The number of oil droplets analyzed was close to 200 for the lowest VOCs (Table 1). For ϕ higher than 10%, the opacity of the mixture increased so that the outline of each droplet was not sharp. Consequently, the number of droplets analyzed was smaller (103 for $\phi = 10\%$ and 84 for $\phi = 60\%$). For $\phi = 80\%$, the diameter of the droplets was not estimated, since they were not spherical. The distribution function of the droplet diameter, which is presented in Figure 3 for each VOC

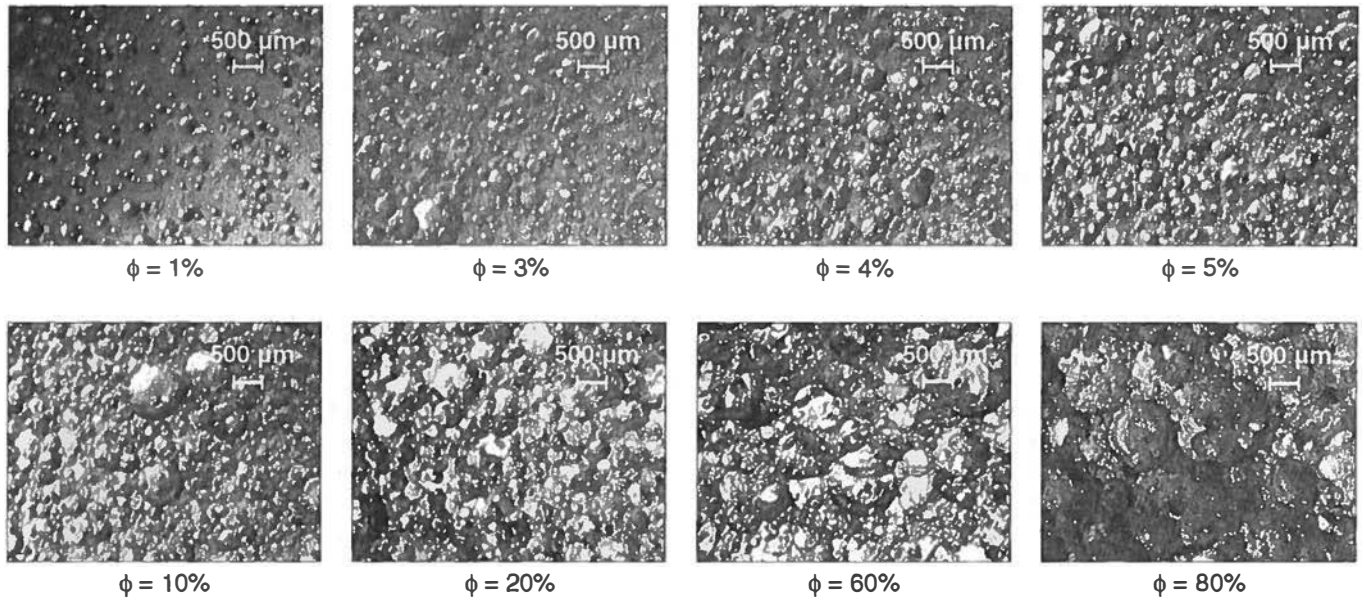


FIGURE 2. Images of the oil-brine mixture at various VOC ϕ for an electrolyte velocity of 1.0 m/s.

TABLE 1
Number, Mean Diameter, and 95% Confidence Interval of the Mean for the Oil Droplets
Analyzed at an Electrolyte Velocity of 1.0 m/s

ϕ (%)	1	2	3	4	5	10	20	60
$N^{(A)}$	172	201	202	186	172	103	89	84
$\langle d_m \rangle^{(B)}$ (μm)	352	369	388	408	445	439	510	698
95% confidence interval	336 to 368	354 to 384	374 to 404	393 to 424	425 to 457	418 to 460	488 to 533	676 to 722

^(A) Number.

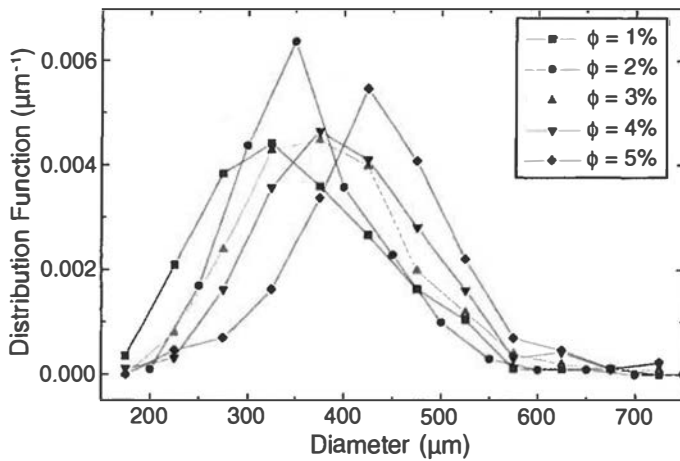
^(B) Mean diameter.

value, is Gaussian and shows a wide scattering of the diameter values. The mean diameter, $\langle d_m \rangle$, and the standard deviation, σ_m , of the distribution were calculated. Figure 4 presents the droplet mean diameter for both electrolyte velocities. The vertical bars indicate the values of d_m ranging between $\langle d_m \rangle - 2\sigma_m$ and $\langle d_m \rangle + 2\sigma_m$. Since d_m follows a Gaussian distribution, 95.4% of the droplet diameters fall within the vertical bars. It must be noticed that for the electrolyte velocity of 1.9 m/s, the shortest aperture time (0.1 ms) of the camera shutter was too long to give sharp pictures of the oil droplets, as shown in Figure 4(b). In these conditions, the distribution function of the droplet diameter could be determined only at the VOC value of 1% and 2% from the individual analysis of 111 and 87 droplets, respectively. Figure 4 shows that the droplet size increased with the VOC and decreased with the electrolyte velocity, which has already been mentioned in the literature for similar conditions.¹³ To confirm the droplet size increase with the VOC, which cannot be clearly seen in Figure 4 because of the high scatter of the diameters at each VOC, the 95% confidence interval of the mean diameter was calculated at each VOC and an analysis of variance (ANOVA) was performed on the whole raw data set for the electro-

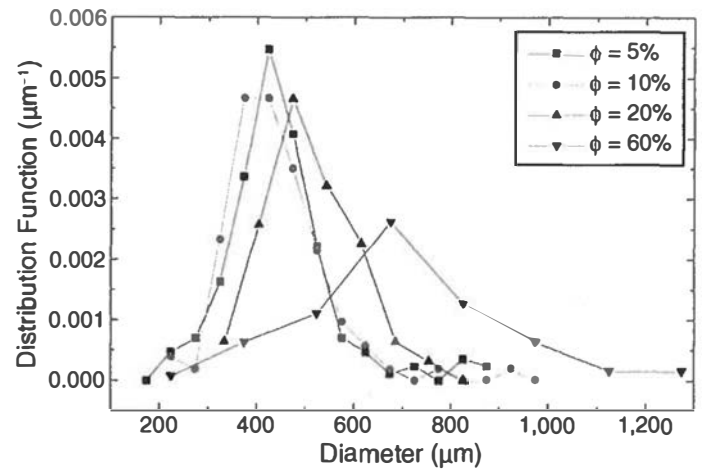
lyte velocity of 1.0 m/s. The results are summarized in Table 1. From both the confidence intervals and the characteristic parameter F of the ANOVA procedure (at the 0.05 level, $F = 107.4$ much larger than 1), it can be concluded that the droplet did increase with the VOC. It can also be observed in Figure 4 that the dispersion of the droplet diameters decreased when the electrolyte velocity increased.

Analysis of the Current Fluctuations

The PSDs of the current fluctuations are shown in Figure 5 for the electrolyte velocities of 1.0 m/s and 1.9 m/s and various values of the VOC. The high-frequency part of the spectra presents several peaks due to the power supply (50 Hz + harmonics) and an increase with the frequency due to the background noise of the ZRA.¹⁴ A plateau can be observed in the low-frequency range, better defined for the high-VOC solutions, followed by a decrease with various slopes. The amplitude of the low-frequency plateau did not change monotonically with the VOC. At the highest electrolyte velocity, it decreased after the addition of small amounts of oil, then increased after further oil additions up to a VOC of 10%, then remained almost constant up to a VOC of 70%. The higher amplitude of

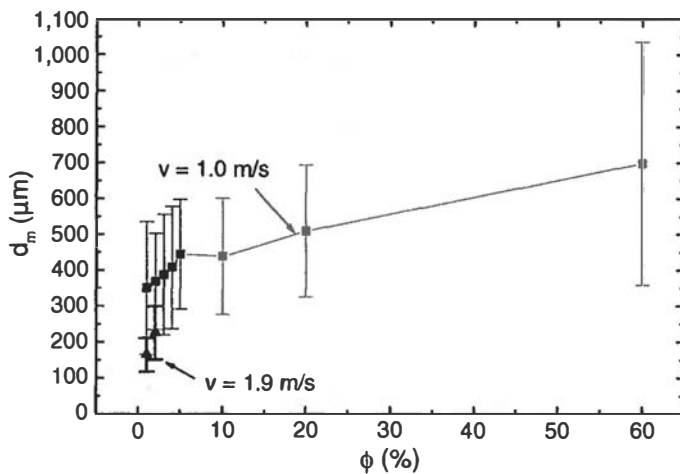


(a)

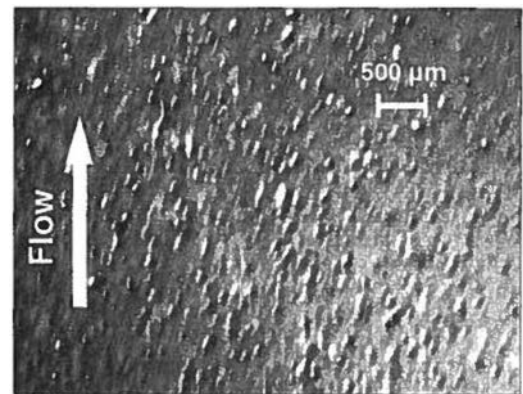


(b)

FIGURE 3. Distribution function of the diameter of the oil droplets at (a) low and (b) high VOC ϕ for an electrolyte velocity of 1.0 m/s.



(a)



(b)

FIGURE 4. (a) Mean diameter of the oil droplets as a function of the VOC for two electrolyte velocities and (b) image of the mixture at $\phi = 1\%$ and $v = 1.9$ m/s.

the plateau at a VOC of 80% was probably due to the first effects of local breakdown of the electrolyte conductivity between the two WEs. At the lowest electrolyte velocity, a certain irreproducibility in the PSD measurements was noticed, which was probably at the origin of the more complex behavior of the PSD amplitude as a function of the VOC. This was caused by an imperfect homogenization of the mixture, as discussed below in the ER measurement section. In all cases, the amplitude of the plateau ranged between $5 \times 10^{-14} \text{ A}^2/\text{Hz}$ and $2 \times 10^{-12} \text{ A}^2/\text{Hz}$. This variation in less than two decades was very close to that observed in the experiments carried out in a cylindrical cell in which the mixture was homogenized with a rotating magnet.^{5,7} The complex behavior and the low sensitivity of the current fluctuations are indications that monitoring corrosion or changes in the hydrodynamic conditions with the current flowing between the WEs would be difficult in practice. Furthermore, the exis-

tence of a low-frequency plateau in the PSDs means that the time records of the current fluctuations present the aspect of a background noise at the commonly used sampling frequencies of 1 Hz or 2 Hz, where no current transient is discernable. This is why the time records are not shown in this paper. In these conditions, the only information available from the time records is the standard deviation, which varies by a factor lower than 10 for ϕ between 0% and 80%.

The interpretation of the shape and amplitude of the PSDs is difficult because of the combined electrochemical and hydrodynamic effects. The at-least partial coverage of the WEs with a dynamic oily phase, which depends on the VOC and on hydrodynamic conditions (flow pattern, flow velocity), controls the corrosion of the iron electrodes. Moreover, the electrochemical activity of the system results from the competition between the enhancement of the cathodic process because of a higher solubility of oxygen in oil

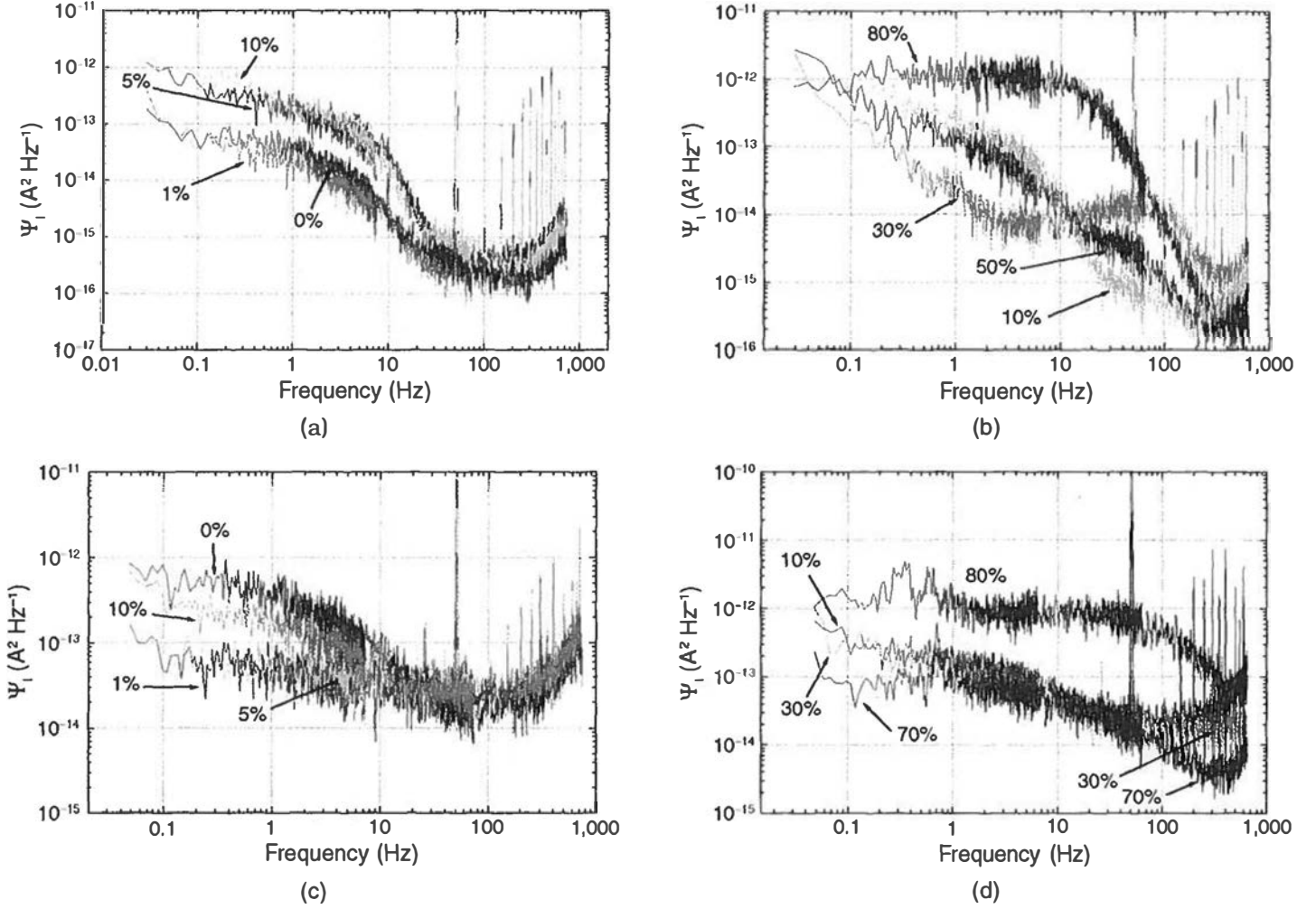


FIGURE 5. PSDs of the current fluctuations measured between two iron WEs at the corrosion potential in an oil-brine mixture with a velocity of (a, b) 1.0 m/s and (c, d) 1.9 m/s at (a, c) low VOC and (b, d) high VOC.

and the metal dissolution inhibition due to the low solubility of the ionic species in oil.

Analysis of the Mean Electrolyte Resistance

The ER is a purely ohmic parameter, the fluctuations of which are directly related to changes in the electrolyte conductivity, induced by changes in the mixture composition between the two WEs, without any contribution of the Faradaic processes on the WEs. Tables 2 and 3 present the mean values $\langle R_e \rangle$ of the ER measured before and after the PSD measurements, which lasted about 20 min, for the two electrolyte velocities investigated and various values of the VOC. The difference in the $\langle R_e \rangle$ values for the solutions with the same low VOC in Tables 2 and 3 (for example, 30.55 Ω and 23.70 Ω at $\phi = 1\%$) comes from the fact that the distance between the two WEs was not the same in the two experiments. A drift with time in the $\langle R_e \rangle$ values can be observed for the lowest electrolyte velocity (Table 2), especially at the low values of ϕ , while the $\langle R_e \rangle$ values are much more stationary for the highest electrolyte velocity (Table 3). A possible explanation of this behavior could be related to a

temperature drift, since the ER is very sensitive to the electrolyte temperature. Indeed, it must be realized that a change of 1°C in temperature corresponds to a change of 2% in the conductivity of the brine solution so that the $\langle R_e \rangle$ drift from 30.55 Ω to 30.31 Ω for $\phi = 1\%$ would correspond to a temperature increase of 0.4°C in 20 min. However, since no $\langle R_e \rangle$ drift was observed in Table 3 for $v = 1.9$ m/s, it is more likely that the variations in the $\langle R_e \rangle$ values in Table 2 are due to an imperfect homogenization of the oil-brine mixture because of an electrolyte velocity that was too low.

The ER mean values can be normalized with the mean value $\langle R_{e,0\phi} \rangle$ measured in the oil-free solution, so that the ratio $\langle R_e \rangle / \langle R_{e,0\phi} \rangle$, which is equal to ρ / ρ_b , where ρ and ρ_b are the electrical resistivities of the mixture and the brine solution, respectively, can be compared to the theoretical ratio given by the Maxwell model of the ionic conduction of a continuous medium (brine) containing dispersed identical spherical particles (oil droplets), expressed as:

$$\frac{\langle R_e \rangle}{\langle R_{e,0\phi} \rangle} = \frac{\rho}{\rho_b} = \frac{1 + \phi / 2}{1 - \phi} \quad (2)$$

TABLE 2
Mean Values of Electrolyte Resistance Measured Before and After the PSD Measurements for an Electrolyte Velocity of 1.0 m/s

ϕ (%)	1	2	3	4	5	10	30	50	80
$\langle R_e \rangle$ (Ω), before	30.55	30.47	30.65	30.41	30.68	32.18	37.44	68.14	129.6
$\langle R_e \rangle$ (Ω), after	30.31	30.36	30.05	30.21	30.81	32.33	36.59	66.72	129.0

TABLE 3
Mean Values of Electrolyte Resistance Measured Before and After the PSD Measurements for an Electrolyte Velocity of 1.9 m/s

ϕ (%)	1	2	3	4	5	30	50	60	80
$\langle R_e \rangle$ (Ω), before	23.70	24.05	24.45	24.82	25.23	35.36	52.75	67.34	142.53
$\langle R_e \rangle$ (Ω), after	23.71	24.10	24.47	24.88	25.29	35.63	52.26	67.40	143.05

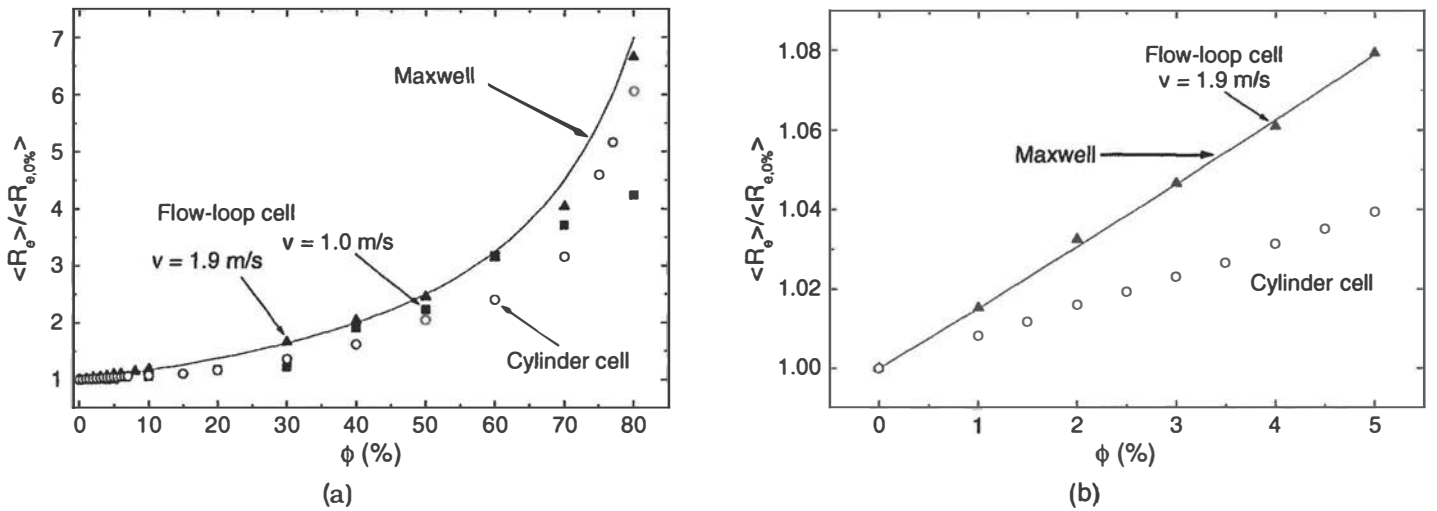


FIGURE 6. Comparison between the normalized mean values of ER and predictions from the Maxwell model (solid line) for experiments in the flow-loop cell, at an electrolyte velocity of (■) 1.0 m/s and (▲) 1.9 m/s, and (○) in the cylinder cell (from Reference 7) at (a) high and (b) low VOC.

$\langle R_e \rangle / \langle R_{e,0\%} \rangle$ is then a linear function of ϕ for small-VOC solutions:

$$\frac{\langle R_e \rangle}{\langle R_{e,0\%} \rangle} = 1 + \frac{3}{2} \phi \quad (3)$$

Figure 6 presents the theoretical and experimental $\langle R_e \rangle / \langle R_{e,0\%} \rangle$ values at high and low VOC for the electrolyte velocity of 1.9 m/s and only at high VOC for the electrolyte velocity of 1.0 m/s because of the $\langle R_e \rangle$ drift. Indeed, Table 2 shows that the $\langle R_e \rangle$ value measured at $\phi = 2\%$ before the PSD measurements is lower than that measured at $\phi = 1\%$, which is not consistent. The $\langle R_e \rangle / \langle R_{e,0\%} \rangle$ values measured in a cylinder cell in which the mixture was stirred with a rotating magnet⁷ are also given in Figure 6 for comparison. In the latter case, the experimental values are lower than the theoretical ones, which was accounted for by the segregation of the two phases in the cylinder cell with a lower VOC close to the WE.

The same behavior was observed in the flow-loop cell at a flow velocity of 1.0 m/s, indicating that the flow was too slow to prevent phase segregation along the flow-loop circuit. The poor reproducibility of the experiments in that case is another indication of the nonuniformity of the oil-droplet concentration in the pipe. On the contrary, for the electrolyte velocity of 1.9 m/s, the agreement between the theoretical and experimental values is excellent, at least up to a VOC value of 60%. The slight differences observed at higher VOC may be due to the fact that the Maxwell model assumes that there is no interaction between the droplets, which is not true for such high VOC values. The good agreement in Figure 6(b) was obtained for the four experiments performed in these conditions. It may be concluded that the electrolyte velocity of 1.9 m/s was sufficiently fast to homogenize the oil-brine mixture perfectly and avoid phase segregation in the pipe. This condition, which allows validation of the Maxwell model for the nonstabilized oil-brine mixture

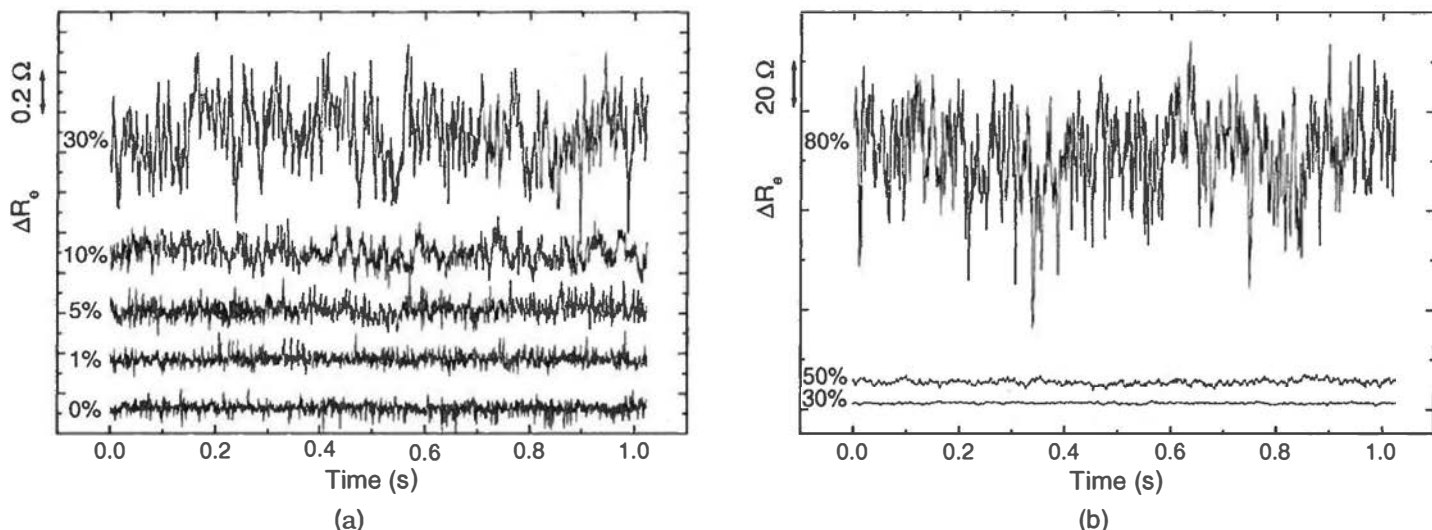


FIGURE 7. Time records of ER fluctuations measured between two iron WEs at the corrosion potential in an oil-brine mixture with a flow velocity of 1.9 m/s at (a) low and (b) high VOC. Arbitrary time scale origin.

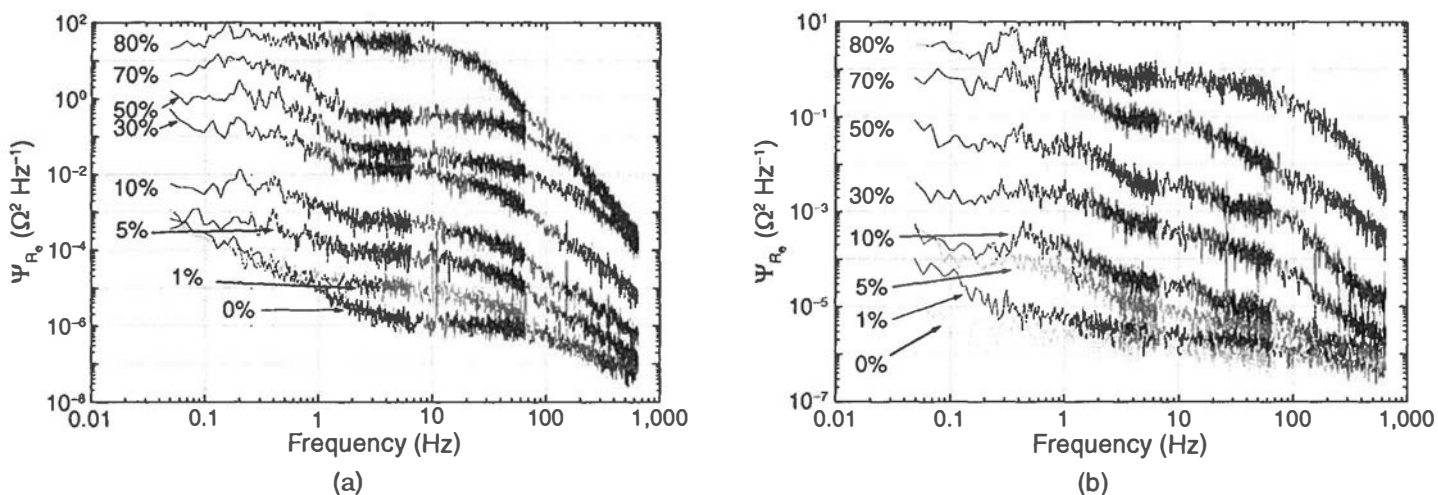


FIGURE 8. PSDs of ER fluctuations measured between two iron WEs at the corrosion potential in an oil-brine mixture of various VOC. Electrolyte velocity: (a) 1.0 m/s and (b) 1.9 m/s.

and validation of the ER measurement, is not fulfilled when the mixture is stirred with a rotating magnet in a cylindrical cell.

Analysis of the Electrolyte Resistance Fluctuations

Figure 7 shows typical time records of the ER fluctuations sampled at 2 kHz for various VOC. The time records sampled at lower frequencies are not shown because they present the aspect of a background noise so that no significant information can be derived from them. The ER fluctuations in the oil-free solution were probably due to the presence of air bubbles circulating in the pipe. As for the previous work,⁷ the ER was found to be very sensitive to the composition of the mixture: the peak-to-peak amplitude varied from 0.1 Ω to 60 Ω when the VOC changed from 0% to 80%. It must be noticed that the

time record at $\phi = 30\%$ was plotted in both Figures 7(a) and (b) to emphasize the large change in the ΔR_e scale.

The large number of oil droplets passing between the WEs per second gives a background noise aspect to the time records because of the overlapping of the ER elementary transients related to the passage of a single droplet. The time-domain analysis was then limited, even at high sampling rates, and, therefore, a frequency-domain analysis was performed. Figure 8 shows the PSDs, $\Psi_{R_e}(f)$, at frequency f of the ER fluctuations calculated for both electrolyte velocities. Once again, the reproducibility of the measurements was not completely satisfying at $v = 1.0$ m/s while it was excellent at $v = 1.9$ m/s. The PSDs present a plateau around 10 Hz and a second plateau appears at low frequency for a VOC higher than 5%. The high-frequency PSD decrease is in $1/f^2$ at low VOC and

$1/f^4$ at the highest VOC. As for the ER time records, it can be seen that the PSDs are very sensitive to the electrolyte composition: the amplitude of the PSD at any frequency increased monotonically with the VOC in a large scale. For example, the amplitude of the high-frequency plateau increased by a factor close to 10^7 for $v = 1.0$ m/s and 10^8 for $v = 1.9$ m/s when the VOC varied from 0% to 80%. For the highest electrolyte velocity, it must be reminded that the PSD of the current fluctuations remained unchanged for VOC ranging between 10% and 70%. On the contrary, $\Psi_{R_e}(f)$ increased by a factor of 10^5 in the same VOC range.

For independent passages of oil droplets, which is a reasonable assumption for the low-VOC solutions, the PSDs of the ER fluctuations can be derived from the theory of the Poisson processes, which concerns processes in which transients independent of one another and occurring at independent random times simply add (like the shot noise in a diode):¹⁵⁻¹⁶

$$\Psi_{R_e}(f) = 2\lambda \langle |\Delta R_e(f)|^2 \rangle \quad (4)$$

where λ is the mean number of droplet passages between the WEs per time unit and $\Delta R_e(f)$ is the Fourier transform of the elementary ER transient $\Delta R_e(t)$ due to the passage of a single droplet:

$$\Delta R_e(f) = \int_0^\infty \Delta R_e(t) e^{-2i\pi f t} dt \quad (5)$$

An extended analysis of the shape and amplitude of $\Psi_{R_e}(f)$ requires the preliminary determination of the elementary transient $\Delta R_e(t)$. Unfortunately, it is quite impossible to identify an elementary ER transient due to the passage of a single droplet even in low-VOC solutions because of the presence of small air bubbles in the pipe. Indeed, Figure 7 shows no difference in the ER fluctuations recorded at $\phi = 0\%$ and $\phi = 1\%$. It is then difficult to determine the mean number of droplets passing between the electrodes or any fundamental information on the size of the droplets from the analysis of the ER fluctuations. For the moment, the ER parameter must be considered only as a very efficient tool for monitoring in real time changes in the composition of a two-phase mixture flowing in a pipe.

To explain the existence of two plateaus in the PSDs, which was not observed when the oil-brine mixture was in a cylindrical cell,^{5,7} it can first be considered that the corresponding elementary ER transient should exhibit two different time constants that would correspond (Figure 8[b]) to the cutoff frequencies of 1 Hz and about 100 Hz (frequencies at which the PSD values are half those of the corresponding plateaus). However, the time necessary for a droplet to pass at a velocity of 1.9 m/s before the WEs of diameter 0.5 cm is about 2.5 ms, which is clearly related to the cutoff frequency of about 100 Hz. On the other hand, it is difficult to imagine a phenomenon associ-

ated with a single oil droplet that would last a few hundreds of milliseconds and could be related to the cutoff frequency of 1 Hz. In this sense, an alternative interpretation of the low-frequency plateau could be the existence of a collective phenomenon, as it was observed in a similar experiment in which silicon carbide (SiC) particles in a sulfuric acid (H_2SO_4) solution, circulating in a pipe at a velocity of 1 m/s or 2 m/s, impinged an iron electrode polarized in the passive domain, which provoked depassivation-repassivation current transients.¹⁷ In that experiment, the PSD of the current fluctuations also presented cutoff frequencies of 1 Hz and 100 Hz, and the low-frequency one could be associated with the variations in time of the mean number λ of SiC particle passages. The Poisson process is termed "doubly stochastic" to indicate that in addition to the random feature of the times of particle passages between the WEs, the passage rate λ was also a random quantity. This was evidenced with the use of a light source and a phototransistor placed on both sides of the pipe: the passage of SiC particles between them provoked fluctuations of the phototransistor current and, although the optical setup was positioned well above the iron electrode, the fluctuations of the electrochemical current and the phototransistor current were perfectly correlated at frequencies lower than 1 Hz. Similar experiments were performed in this work with a 5% VOC mixture circulating at a velocity of 1.9 m/s to evidence a possible correlation between the phototransistor current and the ER signal. The light source and the phototransistor were placed on both sides of the glass pipe at 5 cm above the WEs. All tentatives were unsuccessful; the low-frequency plateau detected on the ER PSD could not be observed on the PSD of the optical signal. However, this does not deny the existence of correlation. The optical arrangement was probably inadequate to sense the passage of each of the very numerous oil droplets correctly. Indeed, all droplets passing simultaneously between the WEs were sensed by the ER signal, while some of them were masked by the outer ones and could not be sensed by the optical signal.

The amplitude of the normalized PSDs $\Psi_{R_e}(f)/\Psi_{R_e,0\%}(f)$ at frequency $f = 10$ Hz, which corresponds to a frequency range in which the PSDs vary slightly, has been plotted in Figure 9 as a function of the VOC for both electrolyte velocities. The normalized PSD values at the low-frequency plateau, $\Psi_{R_e}(0)/\Psi_{R_e,0\%}(0)$, measured in the cylinder cell with the magnetic agitation⁷ are also given. The three curves are similar. Four regions may be distinguished:

- (1) For $\phi \leq 2\%$, the amplitude increases linearly.
- (2) For $2\% \leq \phi \leq 10\%$, the amplitude increases rapidly.
- (3) For $10\% \leq \phi \leq 60\%$, the amplitude increases more slowly.
- (4) For $\phi \geq 60\%$, the amplitude increases rapidly again.

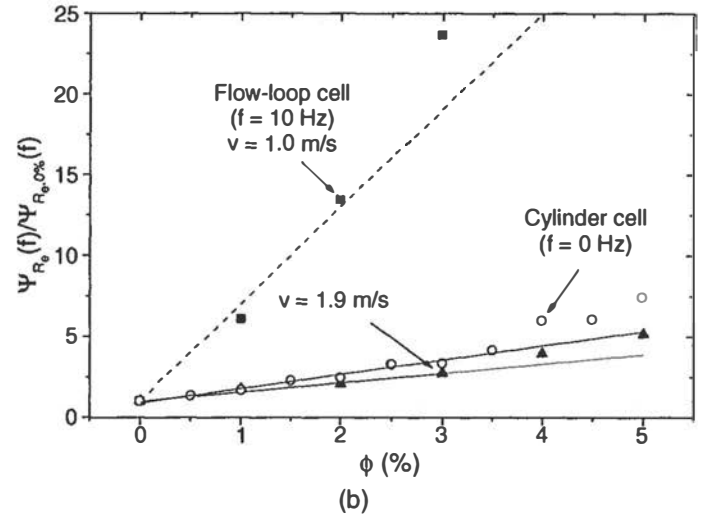
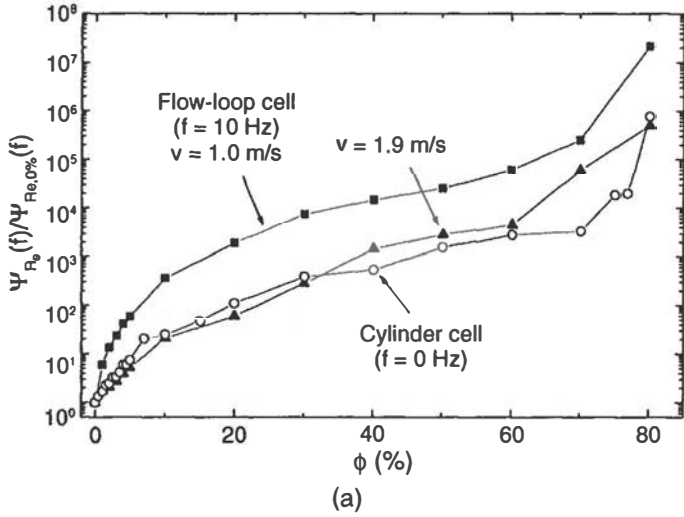


FIGURE 9. Normalized PSDs $\Psi_{R_e}(f)/\Psi_{R_{e,0\%}}(f)$ of ER fluctuations for experiments in the flow-loop cell ($f = 10$ Hz), at electrolyte velocities of (■) 1.0 m/s and (▲) 1.9 m/s (data from Figure 8), and (○) in the cylinder cell ($f = 0$ Hz, from Reference 7) at (a) high and (b) low VOC.

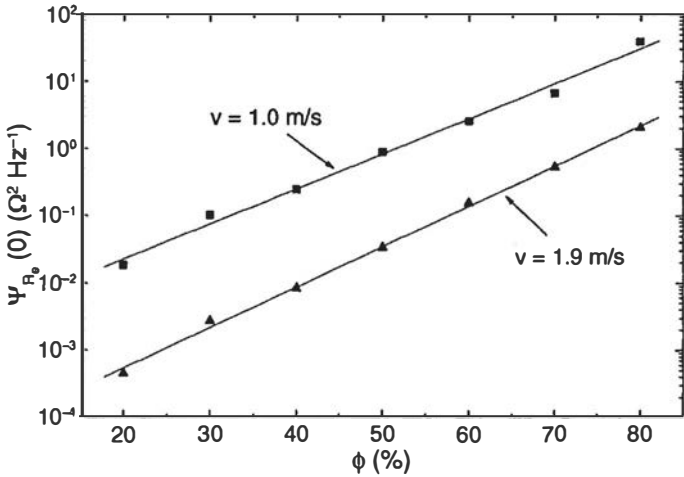


FIGURE 10. Amplitude of the low-frequency plateau of $\Psi_{R_e}(f)$ as a function of the VOC for two electrolyte velocities (data from Figure 8).

These four regions are well defined at the lowest electrolyte velocity, while the regions (2) and (3) overlap in the two other cases. It also can be seen that the PSD amplitude decreased when the electrolyte velocity increased in the flow-loop cell, which means that there are fewer changes in the oily-phase structure between the WEs when the mixture is perfectly homogenized. The PSD values at high velocity in the flow-loop cell are very similar to those measured in the cylinder cell. However, Figure 9(b) shows lower values in the flow-loop cell at low VOC, indicating a still better homogenization of the two phases in that case. This explains why the good agreement between the theoretical and experimental values of $\langle R_e \rangle / \langle R_{e,0\%} \rangle$ could be obtained in the flow-loop cell and not in the cylinder cell. In low-VOC solutions (Figure 9(b)), the linear increase of the amplitude with the VOC (fitting dashed lines) up to 2% for $v = 1.0$ m/s and 3% for $v = 1.9$ m/s is very

similar to that found in the cylinder cell, indicating that the ER fluctuations behave as a Poisson process with independent oil droplets. Figure 10 shows that the amplitude of the low-frequency plateau observed at VOC higher than 20% increased exponentially with the VOC for both electrolyte velocities. This result cannot be explained for the moment.

From the analysis of the diameter of the oil droplets, the expected duration of the elementary transient $\Delta R_e(t)$ induced by the passage of a single droplet between the WEs can be derived. If the current lines between the WEs are considered to be parallel in a cylinder of diameter, $d_c = 0.5$ cm, which is a rough approximation, the time for a droplet passage is $\tau = (d_c + 2 d_m)/v$. As an example, for $v = 1$ m/s and $\phi = 1\%$ ($\langle d_m \rangle = 352 \mu\text{m}$, $\sigma_m = 92.5 \mu\text{m}$), the transient duration is 5.7 ms. The corresponding cutoff frequency of the PSD is close to $1/\tau = 176$ Hz, but it is impossible to calculate its exact value without the knowledge of the shape of the elementary transient. Nevertheless, this value is in the region of the beginning of the PSD decrease at high frequency in Figure 8(a). The cutoff frequency cannot be determined precisely because the PSD is not really flat at mid-frequency. This is likely to be due to the dispersion of the values of τ due to the scattering in the droplet diameters and to the fact that the droplets did not necessarily flow in the direction parallel to the pipe axis between the WEs. A similar reasoning at the electrolyte velocity of 1.9 m/s for $\phi = 1\%$ ($\langle d_m \rangle = 165 \mu\text{m}$, $\sigma_m = 23.3 \mu\text{m}$) gives a value of $1/\tau = 356$ Hz. The PSD does not show any decrease at this frequency because of the importance of the background noise in the oil-free solution, but it is not far from the frequency at which the PSD starts decreasing at higher VOC values in Figure 8(b).

Image analysis has shown the sphericity of the oil droplets up to a VOC of 60%, at least in the vicinity of

the pipe wall. This condition, which was assumed in Maxwell's model of the electrical conduction in two-phase emulsions, may explain the very good agreement obtained in the present work between the model predictions and the experimental values of the mean ER. This confirms the feasibility of an electrolyte-resistance, noise-based sensor for monitoring two-phase electrolyte compositions.

CONCLUSIONS

❖ As already shown in cylindrical cells, the analysis of the electrochemical current noise in flow-loop cells, the hydrodynamic behavior of which is closer to that in pipelines, is not suitable to monitor corrosion of oil-brine mixtures under turbulent hydrodynamic conditions. The current noise data present a complex and nonmonotonic evolution with the VOC that cannot be straightforwardly related to the electrolyte corrosivity or to hydrodynamic features.

❖ On the contrary, the electrolyte-resistance fluctuations yield PSDs showing a reproducible evolution of a 6-decade amplitude with the VOC. This corresponds to a 1,000-fold increase of the amplitude of the ER fluctuations for a VOC ranging from 0% to 80% (WC ranging from 100% to 20%), indicating the feasibility of real-time monitoring of hydrodynamic characteristics and/or fluid composition based on ER noise measurements, which can then be indirectly related to the electrolyte corrosivity. Higher values of VOC induced the intermittent shutdown of the potentiostatic interface control preventing reliable measurements.

❖ In the experimental conditions of the present study, a velocity of 1.9 m/s ensured the dynamic stability of the oil-brine mixture without phase segregation: an excellent agreement was found between the theoretical Maxwell's model of the electrical conductivity of heterogeneous electrolytes containing spherical particles dispersed in a continuum medium. This can also be extremely useful in the in-situ determination of two-phase fluid composition based on real-time ER measurements.

❖ In spite of experimental drawbacks related to the fluid opacity and to the large number of oil droplets,

a video-image analysis was performed. It was shown that the shape of the oil droplets, at least in the vicinity of the pipe wall, was spherical for a VOC up to 60% (WC down to 40%) and that the distribution function of the droplet diameter was Gaussian. The mean diameter of the droplets was determined for all VOC values: it increased with the VOC and decreased when the flow velocity increased.

REFERENCES

1. Y. Chen, M. Gopal, W.P. Jepson, "Comparison of ECN and EIS Measurement for Corrosion Monitoring under Multiphase Flow Conditions," CORROSION/1997, paper no. 276 (Houston, TX: NACE International, 1997).
2. J.M. Malo, J. Uruchurtu, O. Corona, "Corrosion Detection of Mild Steel in a Two-Phase Hydrocarbon-Electrolyte System Under Flow Conditions Using EN," CORROSION/1998, paper no. 381 (Houston, TX: NACE, 1998).
3. J.M. Malo, C.G. Looney, "Recognizing EN Patterns from Mild Steel Corrosion in Oil-Water Mixtures Using Neural Networks," CORROSION/2000, paper no. 472 (Houston, TX: NACE, 2000).
4. T. Hong, Y. Chen, Y.H. Sun, W.P. Jepson, Mater. Corros. 52, 8 (2001): p. 590.
5. F. Huet, R.P. Nogueira, Corrosion 59, 9 (2003): p. 747.
6. H. Wang, "Application of Electrochemical Noise Technique in Multiphase Flow," CORROSION/2005, paper no. 05368 (Houston, TX: NACE, 2005).
7. H. Bouazaze, F. Huet, R.P. Nogueira, Electrochim. Acta 50, 10 (2005): p. 2,081.
8. R.E. Meredith, C.W. Tobias, "Conduction in Heterogeneous Systems," in Advances in Electrochemistry and Electrochemical Engineering, vol. 2, ed. C.W. Tobias (New York, NY: Interscience Publishers, 1962), p. 15.
9. P.J. Sonneveld, W. Visscher, F. Panneflek, E. Barendrecht, M.A.J. Michels, J. Appl. Electrochem. 22, 10 (1992): p. 935.
10. C. Gabrielli, F. Huet, M. Keddam, J. Electrochem. Soc. 138, 12 (1991): p. L82.
11. F. Huet, C. Kuntz, H. Takenouti, "Measurement of Electrolyte Resistance Fluctuations in Corrosion Applications," CORROSION/98, paper no. 378 (Houston, TX: NACE, 1998).
12. U. Bertocci, J. Frydman, C. Gabrielli, F. Huet, M. Keddam, J. Electrochem. Soc. 145, 8 (1998): p. 2,780.
13. M.V. Peralta-Martínez, A. Arriola-Medellín, E. Manzanares-Papayanopoulos, R. Sanchez-Sanchez, E.M. Palacios-Lozano, Petroleum Sci. Technol. 22, 7-8 (2004): p. 1,035.
14. U. Bertocci, F. Huet, J. Electrochem. Soc. 144, 8 (1997): p. 2,786.
15. C. Gabrielli, F. Huet, M. Keddam, R. Oltra, "Localized Corrosion as a Stochastic Process: A Review," in Advances in Localized Corrosion, Proc. 2nd Int. Conf. Localized Corrosion, eds. H.S. Isaacs, U. Bertocci, J. Kruger, S. Smailowska, NACE series, vol. 9 (Houston, TX: NACE, 1990), p. 93.
16. U. Bertocci, F. Huet, B. Jaoul, P. Rousseau, Corrosion 56, 7 (2000): p. 675.
17. R. Oltra, C. Gabrielli, F. Huet, M. Keddam, Electrochim. Acta 31, 12 (1986): p. 1,501.